American Mineralogist, Volume 96, pages 402–407, 2011

The crystal structures and Raman spectra of aravaipaite and calcioaravaipaite

Anthony R. Kampf,[1,*] Hexiong Yang,[2] Robert T. Downs,[2] and William W. Pinch[3]

[1]Mineral Sciences Department, Natural History Museum of Los Angeles County, 900 Exposition Boulevard, Los Angeles, California 90007, U.S.A.
[2]Department of Geosciences, University of Arizona, Tucson, Arizona 85721-0077, U.S.A.
[3]19 Stonebridge Lane, Pittsford, New York 14534, U.S.A.

Abstract

The original structure determination for aravaipaite, $Pb_3AlF_9(H_2O)$, indicated it to be monoclinic, $P2_1/n$, with a = 25.048(4), b = 5.8459(8), c = 5.6505(7) Å, β = 94.013(3)°, V = 829.7(2) Å^3, and Z = 4. Examination of additional crystal fragments from the same specimen revealed that some have a triclinic cell, $P\bar{1}$, with a = 5.6637(1), b = 5.8659(1), c = 12.7041(9) Å, α = 98.725(7)°, β = 94.020(7)°, γ = 90.683(6)°, V = 416.04(3) Å^3, and Z = 2. The topology of the structure is the same as that reported previously, but the structure refinement is significantly improved, with R_1 = 0.0263 for 1695 observed reflections [$F_o > 4\sigma F$] and 0.0306 for all 1903 reflections, and with the H atoms located. Twinning may be responsible for the original monoclinic cell or the two structures could be order-disorder (OD) polytypes.

New X-ray diffraction data collected on a crystal of calcioaravaipaite, $PbCa_2Al(F,OH)_9$, showed it to be triclinic, $P1$, with a = 5.3815(3), b = 5.3846(3), c = 12.2034(6) Å, α = 91.364(2)°, β = 101.110(3)°, γ = 91.525(3)°, V = 346.72(3) Å^3, and Z = 2. This cell is essentially identical to the reduced cell reported in conjunction with an earlier structure solution on a twinned crystal using the OD approach. Our study confirms the findings of the earlier study and significantly improves upon the earlier structure refinement, yielding R1 = 0.0195 for 2257 observed reflections [$F_o > 4\sigma F$] and 0.0227 for all 2427 reflections.

The structures of aravaipaite and calcioaravaipaite are based upon square-packed layers of F atoms on either side of which are bonded Pb atoms (in aravaipaite) or Ca atoms (in calcioaravaipaite) in fluorite-type configurations. These layers parallel to (001) serve as templates to which on both sides are attached AlF_6 octahedra and $PbF_6(H_2O)_2$ polyhedra (in aravaipaite) or PbF_{12} polyhedra (in calcioaravaipaite). The Pb^{2+} cations in these structures have stereoactive $6s^2$ lone-electron-pairs, manifest in off-center coordinations. The very different sizes of the Pb^{2+} and Ca^{2+} cations yield fluorite-type layers with very different metrics, reflected in the a and b cell dimensions of the two structures; but more significantly, the lone-pair effect results in a very irregular template of F atoms peripheral to the fluorite-type layer in aravaipaite, while the F atoms peripheral to the fluorite-type layer in calcioaravaipaite are in a more regular, nearly planar array. As a result, the interlayer AlF_6 octahedra and $PbF_6(H_2O)_2$ polyhedra in aravaipaite form a relatively open configuration, while the AlF_6 octahedra and PbF_{12} polyhedra in calcioaravaipaite form a more tightly packed configuration containing no H_2O molecules.

The Raman spectra of aravaipaite and calcioaravaipaite are consistent with the results of the structure studies, except that the spectrum of calcioaravaipaite exhibits the strong bands typically associated with OH stretching vibrations, while the structure refinement is most consistent with full occupancy of all anion sites by only F.

Keywords: Aravaipaite, calcioaravaipaite, crystal structure, Pb^{2+} $6s^2$ lone-electron-pair, fluorite-type layer structure, order-disorder structure, Raman spectroscopy, Grand Reef mine, Arizona

Introduction

Aravaipaite was originally described by Kampf et al. (1989) from the Grand Reef mine in the Aravaipa mining district of southeastern Arizona. A triclinic cell was reported with a = 5.842(2), b = 25.20(5), c = 5.652(2) Å, α = 93.84(4), β = 90.14(4), γ = 85.28(4)°, V = 827(2) Å^3, and Z = 4; however, polysynthetic twinning on (010) made single-crystal studies difficult and frustrated initial efforts to obtain structure data.

A specimen with larger, superior-quality crystals was later provided for study by one of the authors (W.W.P.). Although these crystals exhibited the same pervasive polysynthetic twinning, a small crystal fragment that appeared to be untwinned provided data that allowed the solution of the crystal structure. The cell derived was monoclinic, $P2_1/n$, with a = 25.048(4), b = 5.8459(8), c = 5.6505(7) Å, β = 94.013(3)°, V = 829.7(2) Å^3, and Z = 4 (Kampf 2001).

Recently, examination of crystals from this same specimen in conjunction with the RRUFF Project (Downs 2006) by one of the authors (H.Y.) determined the long cell dimension to be

* E-mail: akampf@nhm.org

0003-004X/11/0203–402$05.00/DOI: 10.2138/am.2011.3620

half of that reported in the earlier studies. This suggested that the crystal used in the earlier structure determination might actually have been a twin, with the twin law ($\bar{1}00/0\bar{1}0/0.317$ 0.664 1). In the present study, we were successful in separating a small, untwinned crystal fragment, which yielded data for a new structure determination.

In the course of the present study, the crystal structure of calcioaravaipaite, a mineral described from the Grand Reef mine by Kampf and Foord (1996), was also reexamined. The structure of calcioaravaipaite was originally solved by Kampf et al. (2003) using the order-disorder (OD) approach. They determined that their crystal consisted of two twin components of the triclinic maximum degree of order (MDO) polytype, MDO2. To facilitate the OD description of the structure, they used the *C*-centered triclinic cell: a = 7.722(3), b = 7.516(3), c = 12.206(4) Å, α = 98.86(1), β = 96.91(1), and γ = 90.00(1)°. In the present study, we were fortunate to have an untwinned individual, which yielded a significantly improved refinement of the triclinic MDO2 polytype and confirmed the findings of the earlier study. Herein, we have chosen to present the structure in terms of the reduced primitive triclinic cell to facilitate comparison with the structure of aravaipaite.

It is also worth noting that, considering the metrical relationships between the three different cells proposed for aravaipaite (Kampf et al. 1989; Kampf 2001; present study), its structure may also belong to a family of OD structures, in which the triclinic structure presented here and the monoclinic structure described in Kampf (2001) could represent the two MDO polytypes.

Experimental methods

Single-crystal X-ray diffraction data for aravaipaite were obtained on a Rigaku R-Axis Rapid II curved imaging plate microdiffractometer utilizing monochromatized Mo$K\alpha$ radiation. The Rigaku CrystalClear software package was used for processing the structure data, including the application of a numerical (shape-based) absorption correction. The structure was solved by direct methods using SIR92 (Altomare et al. 1994) and the location of all non-hydrogen atoms was straightforward. SHELXL-97 software (Sheldrick 2008) was used, with neutral atom scattering factors, for the refinement of the structure. Bond-valence calculations indicate that the O atom (designated OW) is bonded to two H atoms. A difference Fourier map revealed likely locations for these H atoms. In the final refinement, the positions of H atoms were constrained to an H-OH distance of 0.90(3) Å and an H-H distance of 1.45(3) Å and the isotropic displacement parameters of the H atoms were held constant at 0.05 Å^2.

Single-crystal X-ray diffraction data for calcioaravaipaite were obtained on a Bruker X8 Apex2 CCD diffractometer utilizing monochromatized Mo$K\alpha$ radiation. The data were processed with the Bruker Apex program suite (Bruker 2003), with data reduction using the SAINT program and absorption correction by the multi-scan method using SADABS (Bruker 2003). The structure was solved by direct methods using SHELXL-97 software (Sheldrick 2008) and the location of all atoms was straightforward. SHELXL-97 software was also used, with neutral atom scattering factors, for the refinement of the structure. From electron microprobe and thermogravimetric analyses, Kampf and Foord (1996) derived the empirical formula for calcioaravaipaite $Pb_{1.02}Ca_{2.05}Al_{1.04}[F_{7.97}(OH)_{0.76}O_{0.27}]$ based upon nine anions. This suggests that one of the nine F sites in the structure may be occupied by the O atom of an OH group or that the OH may be spread over two or more F sites. The Raman spectrum (see below) further supports the presence of OH in the structure; however, the best structure refinement was obtained with all anion sites fully occupied by only F and the difference Fourier map revealed no likely sites for H atoms.

The details of the data collections and the final structure refinement for both structures are provided in Table 1. The final atomic coordinates and displacement parameters are listed in Table 2. Selected interatomic distances and angles are listed in Table 3. Bond valences summations are reported in Table 4. Observed and calculated structure factors for aravaipaite and calcioaravaipaite as well as CIFs are available from MSA on deposit[1].

Table 1. Data collection and structure refinement details for aravaipaite and calcioaravaipaite

	Aravaipaite	Calcioaravaipaite
Diffractometer	Rigaku R-Axis Rapid II	Bruker X8 Apex II CCD
X-ray radiation/power	Mo$K\alpha$/50 kV, 40 mA	Mo$K\alpha$/50 kV, 40 mA
Temperature	298(2) K	298(2) K
Structural Formula	$Pb_3AlF_9(H_2O)$	$PbCa_2Al(F,OH)_9$
Space group	$P\bar{1}$	$P\bar{1}$
Unit-cell parameters	a = 5.6637(1) Å	a = 5.3815(3) Å
	b = 5.8659(1) Å	b = 5.3846(3) Å
	c = 12.7041(9) Å	c = 12.2034(6) Å
	α = 98.725(7)°	α = 91.364(2)°
	β = 94.020(7)°	β = 101.110(3)°
	γ = 90.683(6)°	γ = 91.525(3)°
Z	2	2
Volume	416.04(3) Å^3	346.72(3) Å^3
Density	6.686 g/cm^3	4.649 g/cm^3
Absorption coefficient	60.775 mm^{-1}	26.057 mm^{-1}
F(000)	700	432
Crystal size	100 × 45 × 10 μm	40 × 40 × 40 μm
θ range	3.51 to 27.47°	3.40 to 32.63°
Index ranges	$-7 \le h \le 7$	$-7 \le h \le 8$
	$-7 \le k \le 7$	$-8 \le k \le 8$
	$-16 \le l \le 16$	$-18 \le l \le 17$
Reflections coll./unique	14209/1903 (R_{int} = 0.0648)	8559/2427 (R_{int} = 0.0211)
Reflections with $F_o > 4\sigma F$	1695	2257
Completeness to θ = 27.46°	99.6 %	95.9%
Max./min. transmission	0.5816/0.0644	0.4221/0.4221
Refinement method	Full-matrix least-squares on F^2	Full-matrix least-squares on F^2
Parameters refined	135	119
GoF	1.058	1.082
Final R indices ($F_o > 4\sigma F$)	R_1 = 0.0263, wR_2 = 0.0561	R_1 = 0.0195, wR_2 = 0.0412
R indices (all data)	R_1 = 0.0306, wR_2 = 0.0581	R_1 = 0.0227, wR_2 = 0.0419
Extinction coefficient	0.0018(1)	0.0000(3)
Largest diff. peak/hole	+2.066/–2.138 e/Å^3	+2.198/–0.949 e/Å^3

Notes: $R_{int} = \Sigma|F_o^2 - F_o^2(\text{mean})|/\Sigma[F_o^2]$. GoF = $S = \{\Sigma[w(F_o^2 - F_c^2)^2]/(n-p)\}^{1/2}$. $R_1 = \Sigma||F_o| - |F_c||/\Sigma|F_o|$. $wR_2 = \{\Sigma[w(F_o^2 - F_c^2)^2]/\Sigma[w(F_o^2)^2]\}^{1/2}$. $w = 1/[\sigma^2(F_o^2) + (aP)^2 + bP]$ where P is $[2F_c^2 + \text{Max}(F_o^2,0)]/3$; for aravaipaite a is 0.0199 and b is 1.6864; for calcioaravaipaite a is 0.0203 and b is 0.3468.

The crystals of aravaipaite and calcioaravaipaite used in the Raman studies came from the same specimens that yielded the crystals used in the structure studies. Raman spectra were recorded from randomly oriented single crystals on a Thermo Almega microRaman system, using a solid-state laser at 100% power with a frequency of 532 nm and a thermoelectric cooled CCD detector. The laser is partially polarized with 4 cm^{-1} resolution and a spot size of 1 μm.

Description of the structures

The structures of aravaipaite and calcioaravaipaite are shown in Figure 1. Kampf et al. (2003) provided a detailed comparison of the structures and all of their remarks remain valid. Both structures are based upon square-packed layers of F atoms on either side of which are bonded Pb atoms (in aravaipaite) or Ca atoms (in calcioaravaipaite) in fluorite (β-PbF_2)-type configurations. Between these layers, parallel to (001), are located AlF_6 octahedra and $PbF_6(H_2O)_2$ polyhedra (in aravaipaite) or PbF_{12} polyhedra (in calcioaravaipaite). The fluorite-type layers appear to play a critical role in determining the configurations of the interlayer constituents.

The β-PbF_2 layer in aravaipaite

β-PbF_2 has a cubic ($Fm\bar{3}m$) fluorite structure (e.g., Koto et al. 1980) in which each Pb is coordinated to eight F atoms in a

[1] Deposit item AM-11-005, Structure factor and CIF data. Deposit items are available two ways: For a paper copy contact the Business Office of the Mineralogical Society of America (see inside front cover of recent issue) for price information. For an electronic copy visit the MSA web site at http://www.minsocam.org, go to the *American Mineralogist* Contents, find the table of contents for the specific volume/issue wanted, and then click on the deposit link there.

Table 2. Atomic coordinates and displacement parameters (Å²) for aravaipaite and calcioaravaipaite

	x	*y*	*z*	U_{eq}	U_{11}	U_{22}	U_{33}	U_{23}	U_{13}	U_{12}
					Aravaipaite					
Pb1	0.30470(5)	0.11693(5)	0.36471(3)	0.01512(11)	0.01590(17)	0.01373(16)	0.01576(19)	0.00219(12)	0.00129(12)	0.00132(11)
Pb2	0.76753(6)	0.04754(5)	0.11751(3)	0.02400(11)	0.0365(2)	0.01645(18)	0.0190(2)	0.00279(14)	0.00197(16)	–0.00141(14)
Pb3	0.27468(5)	0.51132(5)	0.11789(3)	0.01756(11)	0.01676(17)	0.01772(17)	0.0179(2)	0.00137(13)	0.00200(13)	0.00000(12)
Al	0.7940(4)	0.6181(4)	0.3082(2)	0.0124(5)	0.0098(11)	0.0129(11)	0.0145(13)	0.0022(10)	0.0001(9)	0.0012(8)
F1	0.0486(8)	0.7745(8)	0.2740(4)	0.0265(12)	0.025(3)	0.026(3)	0.027(3)	–0.006(2)	0.013(2)	–0.007(2)
F2	0.7369(8)	0.5094(8)	0.1661(4)	0.0249(11)	0.027(3)	0.033(3)	0.014(3)	0.000(2)	–0.001(2)	–0.002(2)
F3	0.8488(8)	0.7199(9)	0.4455(4)	0.0290(12)	0.024(3)	0.047(3)	0.015(3)	0.001(2)	0.002(2)	0.000(2)
F4	0.5192(8)	0.4752(8)	0.3306(4)	0.0257(12)	0.022(3)	0.025(3)	0.031(3)	0.007(2)	0.001(2)	–0.009(2)
F5	0.6158(8)	0.8676(8)	0.2863(4)	0.0265(12)	0.030(3)	0.019(2)	0.034(3)	0.009(2)	0.013(2)	0.013(2)
F6	0.9587(9)	0.3635(9)	0.3170(5)	0.0394(15)	0.035(3)	0.032(3)	0.052(4)	0.011(3)	–0.005(3)	0.016(2)
F7	0.4996(8)	0.2430(8)	0.9924(4)	0.0188(10)	0.020(2)	0.017(2)	0.019(3)	0.003(2)	0.000(2)	0.0015(18)
F8	0.0007(8)	0.2475(8)	0.9953(4)	0.0176(10)	0.019(2)	0.020(2)	0.013(3)	0.0019(19)	–0.0028(19)	0.0015(18)
F9	0.2942(11)	0.1283(9)	0.1710(4)	0.0407(15)	0.083(4)	0.025(3)	0.014(3)	0.004(2)	0.000(3)	0.000(3)
OW	0.6621(9)	0.2257(9)	0.5128(5)	0.0200(13)	0.013(3)	0.020(3)	0.027(4)	0.000(3)	0.005(3)	0.000(2)
H1	0.597(14)	0.338(13)	0.555(8)	0.050						
H2	0.814(6)	0.253(15)	0.509(8)	0.050						
					Calcioaravaipaite					
Pb	0.27238(3)	0.28211(2)	0.107209(10)	0.01678(5)	0.01998(8)	0.01783(7)	0.01279(7)	–0.00039(4)	0.00367(5)	0.00242(4)
Ca1	0.04213(11)	0.75777(10)	0.61450(5)	0.00876(11)	0.0094(3)	0.0074(2)	0.0095(2)	0.00039(19)	0.0019(2)	0.00025(19)
Ca2	0.44851(11)	0.73503(10)	0.38616(5)	0.00891(11)	0.0092(3)	0.0077(2)	0.0097(2)	0.00065(19)	0.0016(2)	–0.00027(19)
Al	0.20387(18)	0.20662(16)	0.81864(8)	0.00910(16)	0.0098(4)	0.0092(4)	0.0083(4)	0.0006(3)	0.0017(3)	–0.0003(3)
F1	0.8481(5)	0.0489(4)	0.09603(19)	0.0234(5)	0.0285(12)	0.0199(10)	0.0233(11)	0.0075(8)	0.0080(10)	0.0002(8)
F2	0.7419(4)	0.5504(3)	0.27419(17)	0.0165(4)	0.0189(10)	0.0136(8)	0.0195(10)	0.0071(7)	0.0087(8)	0.0030(7)
F3	0.3698(4)	0.0017(3)	0.73490(16)	0.0141(4)	0.0152(9)	0.0125(8)	0.0154(9)	0.0003(7)	0.0045(8)	0.0030(7)
F4	0.0419(4)	0.4057(4)	0.90021(17)	0.0180(4)	0.0219(11)	0.0186(9)	0.0147(9)	–0.0011(7)	0.0058(8)	0.0060(8)
F5	0.9168(4)	0.1103(4)	0.72148(18)	0.0169(4)	0.0117(9)	0.0169(9)	0.0198(10)	–0.0042(7)	–0.0025(8)	0.0011(7)
F6	0.5004(4)	0.2955(4)	0.90746(19)	0.0226(4)	0.0156(10)	0.0273(11)	0.0220(11)	–0.0032(9)	–0.0028(9)	–0.0029(8)
F7	0.2517(4)	0.0076(3)	0.50112(16)	0.0118(3)	0.0122(9)	0.0098(8)	0.0136(9)	0.0011(6)	0.0024(7)	0.0012(6)
F8	0.2503(4)	0.5117(3)	0.50560(16)	0.0116(3)	0.0120(9)	0.0103(8)	0.0130(8)	–0.0002(6)	0.0038(7)	–0.0002(6)
F9	0.2567(4)	0.3857(3)	0.29105(17)	0.0154(4)	0.0185(10)	0.0154(8)	0.0126(9)	–0.0035(7)	0.0051(8)	–0.0043(7)

Table 3. Selected bond distances (Å) and angles (°) for aravaipaite and calcioaravaipaite

			Aravaipaite				
Al-F3	1.760(6)	Pb1-F9	2.469(5)	Pb2-F7	2.462(5)	Pb3-F9	2.443(5)
Al-F6	1.784(5)	Pb1-F5	2.470(5)	Pb2-F8	2.516(5)	Pb3-F8	2.470(4)
Al-F1	1.813(5)	Pb1-F4	2.524(4)	Pb2-F8	2.518(5)	Pb3-F7	2.493(5)
Al-F4	1.819(5)	Pb1-F1	2.542(5)	Pb2-F7	2.530(5)	Pb3-F7	2.548(5)
Al-F2	1.826(6)	Pb1-F6	2.543(5)	Pb2-F2	2.696(5)	Pb3-F8	2.619(4)
Al-F5	1.832(5)	Pb1-F3	2.665(5)	Pb2-F5	2.715(5)	Pb3-F2	2.647(5)
<Al-F>	1.806	Pb1-OW	2.667(6)	Pb2-F9	2.839(6)	Pb3-F1	2.726(5)
		Pb1-OW	2.723(6)	Pb2-F9	3.028(6)	Pb3-F4	2.987(5)
		<Pb1-F>	2.536	Pb2-F6	3.029(6)	Pb3-F2	3.149(5)
		<Pb1-O>	2.695	Pb2-F1	3.104(6)	Pb3-F5	3.263(5)
				Pb2-F2	3.312(5)	Pb3-F6	3.408(6)
				<Pb2-F>	2.795	<Pb3-F>	2.796
			Hydrogen bonds (D = donor, A = acceptor)				
D-H	d(D-H)	d(H···A)	<DHA	d(D···A)	A	<HDH	
OW-H1	0.88(3)	1.85(4)	165(11)	2.713(8)	F4	112(5)	
OW-H2	0.88(3)	1.95(5)	159(10)	2.789(8)	F3		
			Calcioaravaipaite				
Al-F6	1.793(2)	Pb-F9	2.317(2)	Ca1-F9	2.281(2)	Ca2-F9	2.298(2)
Al-F4	1.794(2)	Pb-F4	2.407(2)	Ca1-F8	2.312(2)	Ca2-F8	2.307(2)
Al-F1	1.798(2)	Pb-F1	2.555(2)	Ca1-F7	2.328(2)	Ca2-F7	2.313(2)
Al-F2	1.805(2)	Pb-F6	2.580(2)	Ca1-F2	2.356(2)	Ca2-F5	2.330(2)
Al-F5	1.812(2)	Pb-F4	2.698(2)	Ca1-F7	2.368(2)	Ca2-F8	2.348(2)
Al-F3	1.847(2)	Pb-F6	2.934(2)	Ca1-F8	2.370(2)	Ca2-F3	2.394(2)
<Al-F>	1.808	Pb-F3	2.936(2)	Ca1-F3	2.404(2)	Ca2-F7	2.409(2)
		Pb-F1	2.976(2)	Ca1-F5	2.460(2)	Ca2-F2	2.490(2)
		Pb-F2	3.210(2)	<Ca1-F>	2.360	<Ca2-F>	2.361
		Pb-F5	3.285(2)				
		Pb-F6	3.386(2)				
		Pb-F1	3.399(2)				
		<Pb-F>	2.844				

cube and each F is coordinated to four Pb atoms in a tetrahedral configuration. Recently, β-PbF_2 was found in nature and named fluorocronite (IMA2010-023; Mills et al. 2010). Besides aravaipaite and fluorocronite, three other minerals have structures with layers of the β-PbF_2 structure in which an approximately square-packed array of F atoms is bonded to Pb atoms on either side. One of these is matlockite, PbFCl (Pasero and Perchiazzi 1996), which occurs at numerous localities around the world. The two others, grandreefite (Kampf 1991) and pseudograndreefite (Kampf et al. 1989), also occur at the Grand Reef mine. Grandreefite has also been reported from Lavrion, Greece. The pseudograndreefite structure has not been completely solved, but is known to contain double β-PbF_2 layers (Pb-2F-Pb-2F-Pb); whereas matlockite, aravaipaite, and grandreefite all contain single layers (Pb-2F-Pb), as described above.

As noted by Kampf (2001), the β-PbF_2 layers can be viewed as templates for the organization of the other structural elements. The *a* cell edge in fluorocronite (Mills et al. 2010) is 5.947(3) Å, compared to *a* = 5.66371(12) and *b* = 5.86587(12) Å [with γ = 90.683(6)°] for the layer dimensions in aravaipaite. The smaller dimensions in aravaipaite are made possible by a shift in the positions of the Pb atoms (Pb2 and Pb3) away from the plane of the F atoms (F7 and F8), thereby allowing the F atoms in the layer to be packed closer together.

The Pb2 and Pb3 atoms peripheral to the β-PbF_2 layer are 11-fold coordinated with four short (strong) bonds to F7 and F8 of the square-packed layer and seven irregularly arranged longer bonds to F atoms not in the layer. These Pb atoms are clearly shifted off-center in their coordination environments, as is typical of Pb^{2+} with stereoactive $6s^2$ lone-electron-pairs. The $6s^2$ electrons are directed away from the layer and toward the interlayer region creating a very irregular template of F atoms. As a result, the interlayer AlF_6 octahedra and $PbF_6(H_2O)_2$ polyhedra in aravaipaite form a relatively open configuration.

The CaF_2 fluorite layer in calcioaravaipaite

In calcioaravaipaite, the square-packed layer of F atoms is flanked by Ca atoms yielding CaF_2 fluorite layers in which

TABLE 4. Bond-valence analysis for aravaipaite and calcioaravaipaite

	F1	F2	F3	F4	F5	F6	F7	F8	F9	OW	Sum
						Aravaipaite					
Al	0.485	0.468	0.559	0.477	0.460	0.524					2.973
Pb1	0.251		0.180	0.263	0.304	0.250			0.305	0.238	2.003
										0.212	
Pb2	0.055	0.165			0.157	0.067	0.311	0.269	0.112		1.760
		0.031					0.259	0.267	0.067		
Pb3	0.152	0.189		0.075	0.036	0.024	0.286	0.304	0.328		1.894
		0.049					0.247	0.204			
H1				0.175						0.825	1.000
H2			0.123							0.877	1.000
Sum	0.943	0.902	0.862	0.990	0.957	0.865	1.103	1.044	0.812	2.152	
						Calcioaravaipaite					
Al	0.505	0.495	0.442	0.510	0.486	0.512					2.950
Pb	0.242	0.041	0.086	0.361	0.034	0.226			0.460		1.830
	0.078			0.164		0.087					
	0.025					0.026					
Ca1		0.249	0.219		0.188		0.269	0.281	0.305		1.992
							0.241	0.240			
Ca2		0.174	0.225		0.267		0.280	0.285	0.292		1.994
							0.216	0.255			
Sum	0.850	0.959	0.972	1.035	0.975	0.851	1.006	1.061	1.057		

Notes: Values are expressed in valence units. Pb^{2+}-O bond strengths from Krivovichev and Brown (2001); Pb^{2+}-F bond strengths from Brese and O'Keeffe (1991); Al^{3+}-F and Ca^{2+}-F bond strengths and hydrogen-bond strengths based on H···F bond lengths from Brown and Altermatt (1985).

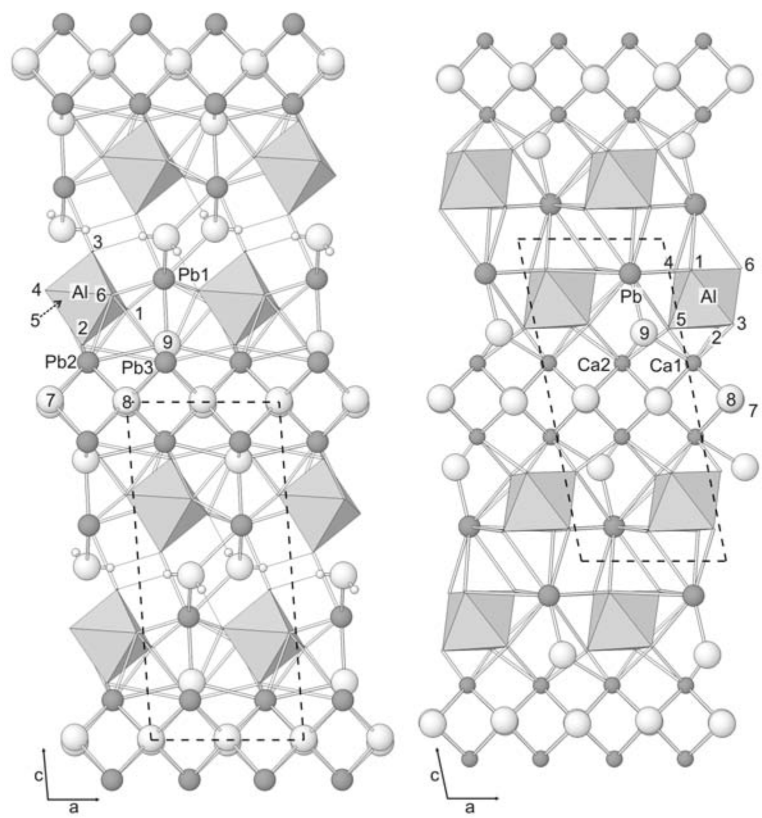

FIGURE 1. Aravaipaite and calcioaravaipaite crystal structures viewed down [010]. The O atoms in aravaipaite are shown as large white spheres bonded to H atoms, shown as small white spheres; the F atoms are numbered 1 through 9.

the two nonequivalent Ca atoms (Ca1 and Ca2) are each eight-coordinated to four F atoms in the fluorite-type layer and four F atoms not in the layer. The Ca1-F bond lengths range from 2.281 to 2.460 Å and the Ca2-F bond lengths range from 2.298 to 2.490 Å. Both coordination polyhedra are regular, slightly twisted cubes. The fluorite layer in calcioaravaipaite thereby provides a much more regular template than the one in aravaipaite resulting in a structure in which all of the F atoms are in well-defined layers parallel to (001). Notably, the AlF_6 octahedra in calcioaravaipaite are oriented such that opposite faces are parallel to (001). The calcioaravaipaite structure is more tightly packed than aravaipaite and contains no H_2O molecules.

The interlayer Pb coordinations

The Pb1 in aravaipaite is only mildly off-center in its eightfold $PbF_6(H_2O)_2$ coordination (Fig. 2). Its $6s^2$ lone-electron-pair appears to be localized approximately opposite the Pb1-F9 bond, directed away from the β-PbF_2 layer and into the interlayer region, between the F3 and two OW ligands.

The Pb in calcioaravaipaite is in unusual 12-fold coordination that represents the first known example of Pb coordinated by 12 F atoms, although some of the F could be OH groups that we were unable to confirm. As noted by Kampf et al. (2003), the coordination polyhedron can be approximately described as a bicapped pentagonal prism. The Pb is markedly off-center with the four shortest Pb-F distances, ranging from 2.317 to 2.580 Å, all on the same side of the polyhedron; the eight longer bonds range from 2.698 to 3.399 Å. The $6s^2$ lone-electron-pair appears to be localized in the interlayer region, directed diagonally away from the β-PbF_2 layer and between the F1-F6 edges of two AlF_6 octahedra (Fig 2).

Raman spectra

The Raman spectra of aravaipaite and calcioaravaipaite, plotted in Figure 3, exhibit strong similarities, especially in the region between 150 and 600 cm^{-1}. This is not surprising, considering the similarities in their structures. Based on previous Raman spectroscopic studies on Al-bearing fluorides (e.g., Rocquet et al. 1985; Brooker et al. 2000; Sosman et al. 2009), the following tentative assignments of observed Raman modes for the two minerals can be made. In Figure 3a, the bands in the frequency regions 200–400 and 400–600 cm^{-1} are associated with the F-Al-F bending (angular deformation) and the Al-F stretching modes of the AlF_6 octahedra, respectively. The two strong peaks between 400 and 600 cm^{-1} for both minerals indicate that there are two distinctive groups of Al-F bond lengths in these minerals, in accord with our X-ray structure analysis data (Table 3). While the bands below 200 cm^{-1} are of a complex nature, primarily due to lattice modes involving Pb-O and Ca-O interactions, as well as AlF_6 octahedral rotations, those between 600 and 700 cm^{-1} are likely to result from the Pb-OH

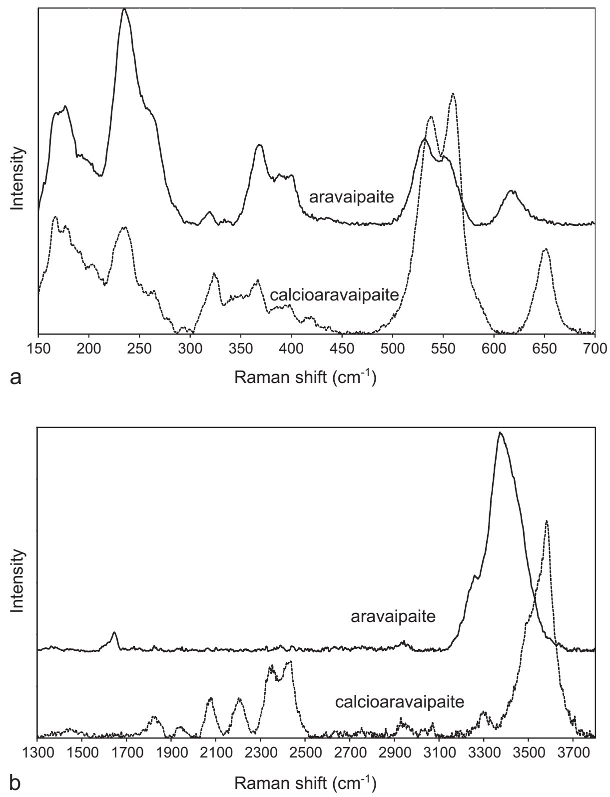

FIGURE 3. Raman spectra of aravaipaite and calcioaravaipaite.

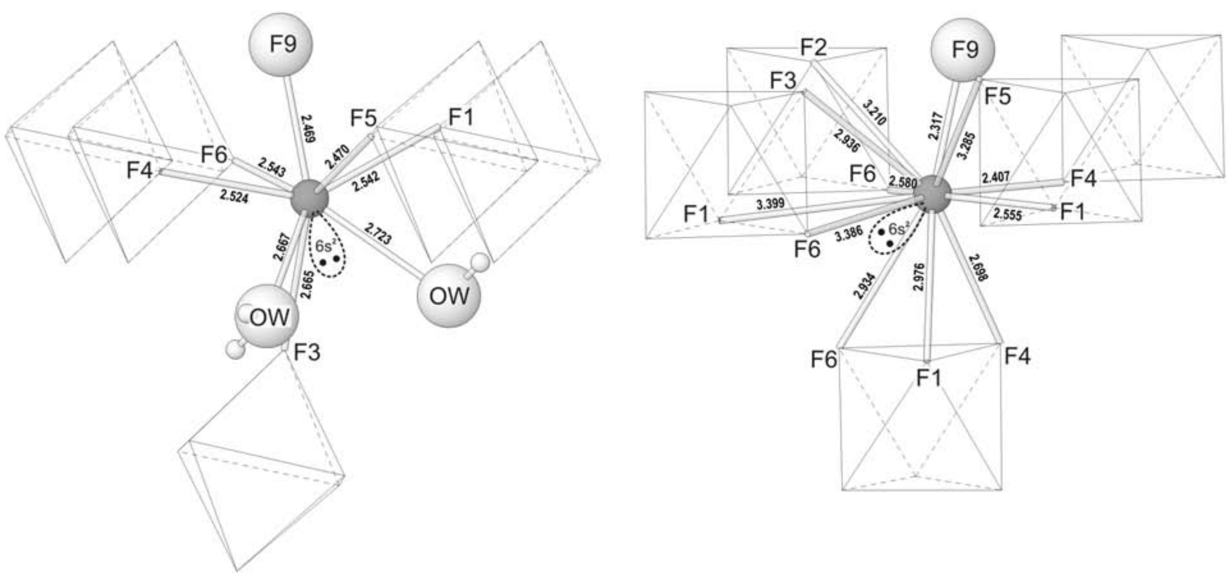

FIGURE 2. The Pb coordinations in the interlayer region in aravaipaite (left) and calcioaravaipaite (right). The AlF_6 octahedra are shown in outline form. The likely approximate locations of the $6s^2$ lone-electron-pairs are shown. In each case, the fluorite-type layer is toward the top of the image.

(for avaraipaite) or (Ca,Pb)-OH (for calcioaravaipaite) bending modes. Such M-OH bending modes have been observed in many hydrous oxides, such as diaspore AlO(OH), goethite FeO(OH), brucite $Mg(OH)_2$, and portlandite $Ca(OH)_2$ (e.g., de Faria et al. 1997; Ruan et al. 2001; Braterman and Cygan 2006), and their frequencies appear to increase with increasing M-O bond strength for materials with similar structures. Our Raman spectroscopic data agree with this observation. For aravaipaite, the M-OH bending mode is at ~617 cm^{-1}, which should be related to the two Pb1-OW bonds (with the bond lengths of 2.667 and 2.723 Å; Table 3). For calcioaravaipaite, nevertheless, this mode appears at ~652 cm^{-1}. The marked shift of the peak position to a higher frequency relative to that for aravaipaite can be accounted for by the fact that all of the F sites in calcioaravaipaite participate in at least one bond with a shorter distance. The position of this peak can be used to distinguish the two mineral phases using Raman spectroscopy.

Both aravaipaite and calcioaravaipaite display strong bands between 3100 and 3700 cm^{-1} (Fig. 3b) that are associated with the OH stretching vibrations. Although we are not certain about the nature of bands between 1900 and 3100 cm^{-1} for calcioaravaipaite (though they are consistent with typical fluorescence peaks associated with trace element substitutions in Ca sites), the small bands between 1580 and 1680 cm^{-1} for aravaipaite can be assigned to the H-O-H bending vibrations, which are typical of materials containing H_2O molecules. The existence of OH in calcioaravaipaite, as revealed by our Raman spectroscopic measurements, evidently lends support to the chemical formula for this mineral proposed originally by Kampf and Foord (1996) and Kampf et al. (2003) as $PbCa_2Al(F,OH)_9$, rather than that recorded in the current IMA list as $PbCa_2AlF_9$, although assuming that OH is not dominant at any anion site, the latter does represent the end-member formula. More detailed research is apparently needed to address whether OH in calcioaravaipaite is an essential component or just a substitution for F at one or two of the anion sites.

Acknowledgments

Reviewers Stuart J. Mills and Marco Pasero are acknowledged for helpful comments on the manuscript, and the latter is particularly thanked for comments on the OD character of these minerals. This study was funded by the John Jago Trelawney Endowment to the Mineral Sciences Department of the Natural History Museum of Los Angeles County, and by the Science Foundation Arizona.

References cited

Altomare, A., Cascarano, G., Giacovazzo, C., Guagliardi, A., Burla, M.C., Polidori, G., and Camalli, M. (1994) SIR92—A program for automatic solution of crystal structures by direct methods. Journal of Applied Crystallography, 27, 435.

Braterman, P.S. and Cygan, R.T. (2006) Vibrational spectroscopy of brucite: A molecular simulation investigation. American Mineralogist, 91, 1188–1196.

Brese, N.E. and O'Keeffe, M. (1991) Bond-valence parameters for solids. Acta Crystallographica, B47, 192–197.

Brooker, M.H., Berg, R.W., von Barner, J.H., and Bjerrum, N.J. (2000) Raman Study of the hexafluoroaluminate ion in solid and molten FLINAK. Inorganic Chemistry, 39, 3682–3689.

Brown, I.D. and Altermatt, D. (1985) Bond-valence parameters obtained from a systematic analysis of the Inorganic Crystal Structure Database. Acta Crystallographica, B41, 244–247.

Bruker (2003) SAINT, SADABS and SHELXTL. Bruker AXS Inc., Madison, Wisconsin.

de Faria, D.L.A., Silva, S.V., and de Oliveira, M.T. (1997) Raman microspectroscopy of some iron oxides and oxyhydroxides. Journal of Raman Spectroscopy, 28, 873–878.

Downs, R.T. (2006) The RRUFF Project: an integrated study of the chemistry, crystallography, Raman and infrared spectroscopy of minerals. Program and Abstracts of the 19th General Meeting of the International Mineralogical Association in Kobe, Japan, O03-13.

Kampf, A.R. (1991) Grandreefite, $Pb_2F_2SO_4$: Crystal structure and relationship to the lanthanide oxide sulfates, $Ln_2O_2SO_4$. American Mineralogist, 76, 278–282.

——— (2001) The crystal structure of aravaipaite. American Mineralogist, 86, 927–931.

Kampf, A.R. and Foord, E.E. (1996) Calcioaravaipaite, a new mineral, and associated lead fluoride minerals from the Grand Reef mine, Graham County, Arizona. Mineralogical Record, 27, 293–300.

Kampf, A.R., Dunn, P.J., and Foord, E.E. (1989) Grandreefite, pseudograndreefite, laurelite, and aravaipaite: Four new minerals from the Grand Reef mine, Graham County, Arizona. American Mineralogist, 74, 927–933.

Kampf, A.R., Merlino, S., and Pasero, M. (2003) OD approach to calcioaravaipaite, [$PbCa_2Al(F,OH)_9$]: The crystal structure of the triclinic MDO polytype. American Mineralogist, 88, 430–435.

Koto, K., Schulz, H., and Huggins, R.A. (1980) Anion disorder and ionic motion in lead fluoride beta-PbF_2. Solid State Ionics, 1, 355–365.

Krivovichev, S.V. and Brown, I.D. (2001) Are the compressive effects of encapsulation an artifact of the bond valence parameters? Zeitschrift für Kristallographie, 216, 245–247.

Mills, S.J., Kartashov, P.M., Gamyanin, G.N., Whitfield, P.S., Kern, A., Guerault, H., and Raudsepp, M. (2010) Fluorocronite, IMA2010-023. CNMNC Newsletter 4, 2010, p. 799; Mineralogical Magazine, 74, 797–800.

Pasero, M. and Perchiazzi, N. (1996) Crystal structure refinement of matlockite. Mineralogical Magazine, 60, 833–836.

Rocquet, P., Couzi, M., Tressaud, A., Chaminade, J.P., and Hauw, C. (1985) Structural phase transition in chiolite $Na_5Al_3F_{14}$: I. Raman scattering and X-ray diffraction study. Journal of Physics, C: Solid State Physics, 18, 6555–6569.

Ruan, H.D., Frost, R.L., and Kloprogge, J.T. (2001) Comparison of Raman spectra in characterizing gibbsite, bayerite, diaspore and boehmite. Journal of Raman Spectroscopy, 32, 745–750.

Sheldrick, G.M. (2008) A short history of SHELX. Acta Crystallographica, A64, 112–122.

Sosman, L.P., Yokaichiya, F., and Bordallo, H.N. (2009) Raman and magnetic susceptibility study of hexagonal elpasolite Cs_2NaAlF_6: Cr^{3+}. Journal of Magnetism and Magnetic Materials, 321, 2210–2215.

Manuscript received June 8, 2010
Manuscript accepted September 14, 2010
Manuscript handled by Diego Gatta